ELSEVIER

Journal of Chromatography A, 769 (1997) 37–48

JOURNAL OF CHROMATOGRAPHY A

Simple model for blending aqueous salt buffers Application to preparative chromatography

O. Kaltenbrunner, A. Jungbauer*

Institute for Applied Microbiology, University of Agriculture, Forestry and Biotechnology, Nussdorferlände 11, A-1190 Vienna, Austria

Abstract

In preparative chromatography of proteins and other biopolymers, elution is frequently achieved by a stepwise or continuous change of the mobile phase composition, generally denoted as step or linear gradient. The gradient is formed by inline mixing of two aqueous buffers. For prediction of peak profiles, examination of the reliability of blending devices and remote control of chromatography controllers a model would be advantageous. This would be most beneficial for ion-exchange chromatography and hydrophobic interaction chromatography where aqueous buffers must be blended. Here different salt concentrations are commonly blended. The model is able to describe the delay of onset and the transition period for step gradient. We developed a model based on the simple continuously stirred tank reactor model (CSTR) which has been modified to include logistic growth. Two parameters have to be estimated; parameter a is a lumped parameter related to the exponential time constant and Gaussian broadening. The second parameter, denoted b, describes the delay inherent to the system. This novel model is compared to a model based on the convolution of a step input with a Gaussian broadening and an exponential decay. The predicted values of both models are similar, when compared to experimental data obtained from inline mixing of two salt buffers. The logistic growth modified CSTR model exhibited higher residuals than the convolution model. The beginning of the gradient cannot be approximated in a smooth fashion, since the applied equation contains a sharp inflection. The current model's application is limited to the blending of salt buffers; pH is not a consideration of this model.

Keywords: Gradient elution; Logistic growth; Mobile phase composition; Salt gradients; Preparative chromatography; Continuously stirred tank reactor model

1. Introduction

In preparative and analytical chromatography elution is frequently effected by linear, step and segmented gradients. Aqueous buffers are very common in ion-exchange, hydrophobic interaction and affinity chromatography [1]. The elution buffer is generally mixed from at least two buffers differing in salt concentration or pH. Considering a binary gradient, two displacement pumps operated by remote controller deliver the buffer solutions. A less desirable alternative is a single pump operated with a proportioning valve. In either case the percentage of the buffer ions finally presented in the elution buffer is determined by the ratio of the pump's velocity or the valve's position, since the flow-rate must be kept constant. Both liquid streams must be thoroughly mixed. This is normally accomplished by small stirrers or a passive bubble trap. The streams are introduced into a small stirred vessel and subsequently drained through a third pipe. In commercially available equipment the stirrer speed cannot be adjusted. The pipe (tube) diameter is fixed, or can be varied only within a small range. Thus, the volume

*Corresponding author.

PII S0021-9673(97)00161-1

of the mixing chamber is also fixed in most cases [2,3]. These compromises are accepted by end-users. Although not ideal, systems are designed in this manner for handiness and simplicity. A switch valve, metering the required amount of buffers, is also used by some manufacturers of chromatography equipment. The considerations made here do not refer to this mode of buffer blending.

There are no current models which predict salt gradients for commonly employed mixing devices. Several assumptions must be made for development of a model. Our model will presume that there is no chemical reaction between the buffers. It will also assume that volume contraction is negligible after mixing. Our assumption is that the mixing enthalpy is very low and the process can be regarded as isothermal. Our model also presumes that both buffers are miscible without a miscibility gap. The mixing chamber is thought to be a stirred vessel and all mixing will occur in this vessel.

One approach of rapid optimization of preparative chromatography is achieved by utilizing computer assisted methods [4,5]. These approaches require models for broadening and retention in the column [4,6,7] and extra-column broadening. While the focus of a preceding paper was on the extra column broadening of the protein band [8], this paper is on system inherent effects of gradient generation. Our contention is that the actual gradient influences the retention, and thereby the chromatogram's shape. In preparative chromatography the ideal and actual gradients may be quite different. Thus a function predicting this time dependent change of the elution buffer's salt concentration is required. Glajch and Snyder [5] have neglected this deviation from the ideal form. They only considered the delay, expressed by the dwell volume. In practice, the linear and step gradient are modified to an asymmetrical S-shaped curve.

It is apparent to describe the response function of a mixing device for a step input simply by a function for a continuously stirred tank reactor (CSTR) convoluted with a Gaussian broadening. For other shapes of the input function like linear gradients and segmented gradients the same approach is applicable but not as simple. Therefore, a simplified model was established and compared to the mathematically more rigorous approach. The simplified model is based on exponential wash out. These functions have been expanded by functions for logistic growth.

2. Theory

The more rigorous mathematical treatment is based on the convolution integral method described by Sternberg [9]. A function describing the gradient profile has been developed by convolution of a step input signal, an exponential decay function and a Gaussian distribution (Fig. 1).

The convolution of a step input and an exponential decay function is

$$f(t) = 1 - \exp\left(-\frac{t-\tau_r}{\tau_e}\right), \quad \text{if } t > \tau_r$$
$$f(t) = 0, \quad \text{if } t \leq \tau_r \tag{1}$$

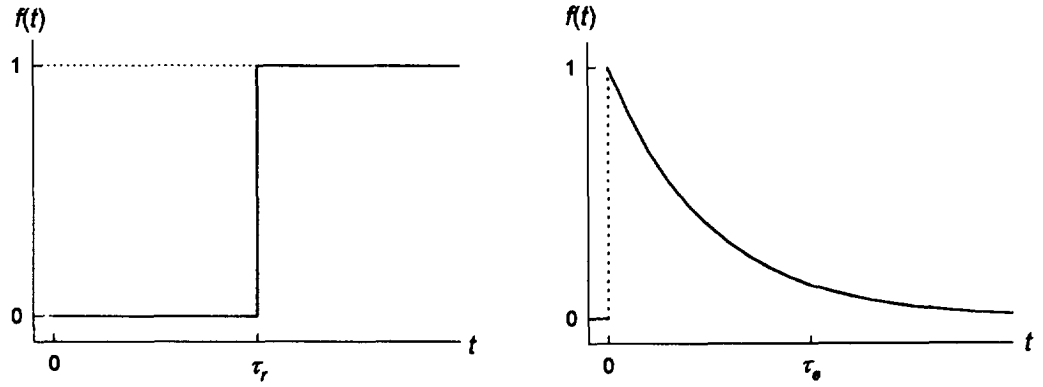

Fig. 1. Schematical drawing of step and exponential decay function. Nomenclature according to Eqs. (1–4).

Using Eq. (1) as an input function of the convolution integral

$$g(t) = \frac{1}{\sqrt{2 \cdot \pi} \cdot \sigma} \cdot \int_{\text{all values of } x} f(x) \cdot \exp\left[-\frac{(t-x)^2}{2 \cdot \sigma^2} \right] dx \quad (2)$$

leads to

$$g(t) = \frac{1}{\sqrt{2 \cdot \pi} \cdot \sigma} \cdot \int_{t_R}^{\infty} \left[1 - \exp\left(-\frac{x}{\tau_e} \right) \right] \cdot \exp\left[-\frac{(t-x)^2}{2 \cdot \sigma^2} \right] dx \quad (3)$$

The integration of Eq. (3) gives

$$f(t) = \frac{1}{2} \cdot \left\{ \exp\left(\frac{\sigma^2}{2 \cdot \tau_e^2} - \frac{t - t_R}{\tau_e} \right) \cdot \left[\operatorname{erf}\left(\frac{\sqrt{2} \cdot \sigma}{2 \cdot \tau_e} - \frac{\sqrt{2} \cdot (t - t_R)}{2 \cdot \sigma} \right) - 1 \right] + \operatorname{erf}\left(\frac{\sqrt{2} \cdot (t - t_R)}{2 \cdot \sigma} \right) + 1 \right\} \quad (4)$$

The parameter values for σ (Gaussian broadening) and τ_e (exponential contribution to broadening) of the extra column space of the system are obtained by fitting of breakthrough curves using Eq. (4). The breakthrough must be done with an empty column. The adapters of the inlet and outlet of the column are put together such, that there is no dead volume between the adapters.

The derivative of this equation is an exponentially modified Gaussian distribution. Therefore, the statistical moments of the distribution are easily found using a moment vector (M) [10–13].

$$M = \begin{bmatrix} m'_1 \\ m_2 \\ m_3 \\ m_4 - 3 \cdot m_2^2 \end{bmatrix} = \begin{bmatrix} t_m + \tau_e \\ \sigma^2 + \tau_e^2 \\ 2 \cdot \tau_e^3 \\ 6 \cdot \tau_e^4 \end{bmatrix} \quad (5)$$

So, an analysis of the breakthrough data including variance (m_2) skewness (S)

$$S = \frac{m_3}{m_2^{3/2}} \quad (6)$$

and excess (E) of the distribution is well achievable.

$$E = \frac{m_4 - 3 \cdot m_2^2}{m_2^2} \quad (7)$$

Difficulties arise when gradient shapes other than steps are used. Therefore, this function is of limited usefulness. For example in the case of a linear gradient, a ramp function has to be convoluted with an exponential decay function and a Gaussian broadening function. For segmented gradients various combinations of ramp and step functions have to be combined. It seems to be very difficult to predetermine all possible combinations of gradients a commercially available gradient controller can apply to a chromatographic system.

Thus, a simplified approach based on the description of the continuous stirred tank reactor (CSTR) was developed. The stirred tank definition

$$\frac{dI}{dt} = \frac{1}{a} \cdot I \quad (8)$$

limits the possibilities of various user-defined gradient shapes. Here a is the time constant of the mixer and I is the salt concentration. When this function is applied for the description of a breakthrough curve of a chromatographic system without packing material a is a lumped parameter of exponential time constant and Gaussian broadening. To enable description of all different kinds of linear and segmented gradients, the following model for logistic growth can be utilized.

$$\frac{dI}{dt} = \frac{1}{a} \cdot I \cdot \left(1 - \frac{I}{I_{max}} \right) \quad (9)$$

Using this function, different salt gradients can be described by varying the value for I_{max}. The explicit solution of integrating between I_0 and I_{max} gives

$$I = \frac{I_0 \cdot I_{max} \cdot \exp\left(\frac{t}{a} \right)}{\exp\left(\frac{t}{a} \right) + I_{max} - I_0} \quad (10)$$

This equation can be used to determine the lumped constant a of the function.

The range of the gradient is normalized between 0 and 1 for curve-fitting and the additional term (b) is added to describe the delay inherent in the system. Thus, the function is modified to

$$I = 0 \qquad \text{for } t \leq b$$

and

$$I = \frac{2 \cdot \exp\left(\frac{t-b}{a}\right)}{\exp\left(\frac{t-b}{a}\right) + 1} - 1 \qquad \text{for } t > b \tag{11}$$

This function can be used to fit step gradients. In this regard, the parameter a acts as a time constant and should be comparable to τ_e in Eq. (4) and b is a delay time (volume) and should be comparable to t_D (V_D) in Eq. (4). Insertion of parameter a in Eq. (9) in conjunction with the value of I_{max} (to control the gradient shape) differently shaped gradients can be described by this equation.

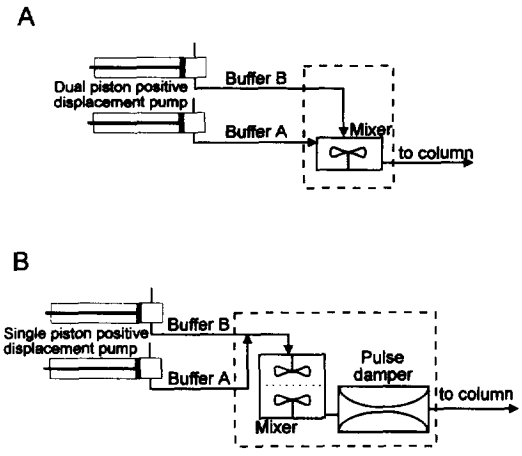

Fig. 2. Schematic drawing of the high-pressure mixing systems applied. (A) Inline mixer as normally used in an HPLC-system. To provide best mixing effect, the line with the buffer of higher density enters the mixer from the top while the less dense buffer is pumped in radial. (B) Inline mixer as normally used in a ProSys Workstation. Two mixers are connected together in series. They are separated by a seal with several bores. Both solutions are pumped radial into the first mixer and are leaving the system from the second. Dashed lines are the virtual system, which is thought to be a stirred vessel.

3. Experimental

3.1. Apparatus

Two chromatographic systems were used. First, denoted as HPLC, two high-performance pumps P-3500 (Pharmacia Biotech, Uppsala, Sweden) were controlled by a liquid chromatography controller LCC-500 plus (Pharmacia Biotech). These pumps are dual piston displacement pumps. They do not require a pulse dumper. The tubings from the pumps were connected to a mixer 24V (Pharmacia Biotech), a dynamic mixer of 0.6 ml volume (Fig. 2A). The system effluent was monitored by a conductivity monitor (Pharmacia Biotech). The analog signals were transferred to a PE Nelson 900 Series Interface and stored digitally by a Model 2600 Chromatography Software, Rev. 4.1 (Nelson Analytical, Cupertino, CA, USA). The sample was loaded by a P-3500 pump.

Second, a ProSys Chromatography System (BioSepra, Marlborough, MA, USA) was used. The pump module contains 4 single piston pumps delivering up to 30 ml/min each and a mixing devices to allow buffer blending from up to 4 stock solutions. The tubings from the pumps are connected to two dynamic mixers in series (only separated by a seal) of 1.2 ml volume (Fig. 2B). The separation module consists of a pH monitor, a conductivity monitor, and an A/D converter with software controlled data rates from 0.1 to 10 Hz. The whole system is controlled by a ProSys Workstation installed on a 486/66 CPU with 8 Mbytes Ram.

3.2. Buffers

For all experiments, a 10 m*M* Tris–HCl buffer pH 8.0 and a 10 m*M* Tris–HCl buffer pH 8.0 containing 1 *M* NaCl were used.

3.3. Numerical treatment of data

Raw data from the chromatograms are exported from the Nelson data acquisition software and the ProSys workstation to all other programs as tab-delimited textfiles. Curve-fitting was carried out by using the software TableCurve 2D and TableCurve 3D (Jandel Scientific, San Rafael, CA, USA). Multiple linear regressions were carried out using SigmaStat (Jandel Scientific).

For the calculation of Eq. (4), error functions are needed. They were approximated according to Abromowitz and Stegun [14].

4. Results

When step-gradients are produced by a two-pump system with a mixer, S-shaped curves can be observed. Normalized gradients in respect to the maximal salt concentration (made out of the same stock solutions) allow quantitative comparison and evaluation of the salt profiles. Superimposing all normalized profiles (Fig. 3) demonstrate a slight shift of the ascent with the maximum salt concentration both for ProSys and HPLC.

This observation indicates, that the shape and ascent–delay of the step gradient is highly related to the maximal salt concentration, denoted as transition height. Furthermore shape and delay are also dependent on the flow-rate.

Prior to the prediction of the gradient by the equations derived in the Section 2, several parameters must be determined. This can be accomplished by breakthrough curves. They were created using a column with connected adapters. The salt step has been applied and the conductivity response curve is measured. The conductivity meter has been calibrated in order to have a linear response between salt concentration and the signal. These experiments were carried out with different flow-rates and different transition heights. The response curves were fitted with both models (Eq. (4) and Eq. (11)). The time axis was converted to a volume axis in order to compare normalized gradients produced by different flow-rates. The delay volume V_D is calculated by $t_D \cdot F$.

Both models could adequately fit the response curve, while the description of the data by the model based on the convolution integral method is better (Fig. 4). The residuals are smaller and positive and negative residuals are present in the same quantity.

Fitting of Eq. (4) to experimental breakthrough curves at different flow-rates and different transition heights allows an analysis of influences of these parameters on the system response by means of σ and τ_e. Therefore experiments at different transition heights (from 0.0 *M* NaCl to 0.1; 0.25; 0.5; 0.75 and 1.0 *M* NaCl) (Fig. 3) and various flow-rates (1.0; 2.0; 4.0 and 8.0 ml/min) were carried out (Fig. 5).

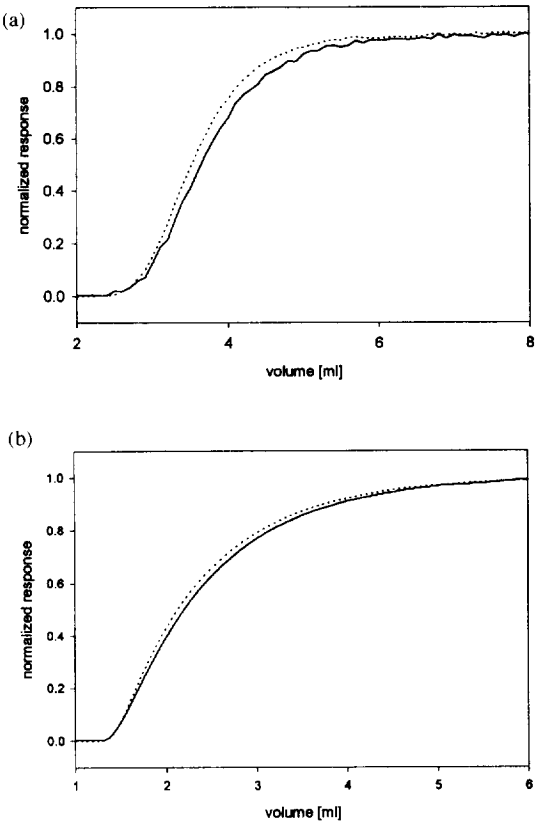

Fig. 3. Normalized gradients with respect to maximum salt concentration (I_{max}). (a) Profiles from a transition height of 0.1 (———) and 1 *M* salt (· · ·) produced using a ProSys Workstation are superimposed. The flow-rate for all experiments was kept constant at $F = 2.0$ ml/min. (b) Profiles from a transition height of 0.2 (———) and 1 *M* salt (· · ·) produced using HPLC are superimposed. The flow-rate for all experiments was kept constant at $F = 1.0$ ml/min.

Fig. 5 shows the shift of the salt profile with different flow-rates at a fixed transition height. Multiple linear regressions were performed for a more accurate evaluation. As independent variable transition height and flow-rate has been chosen, since their influence on the gradient formation should be revealed. According to Eq. (4), the convolution integral method, delay volume V_D, Gaussian broadening σ and exponential decay are the parameters influencing the shape of the function (Fig. 6a–c). Furthermore the statistical moments were derived

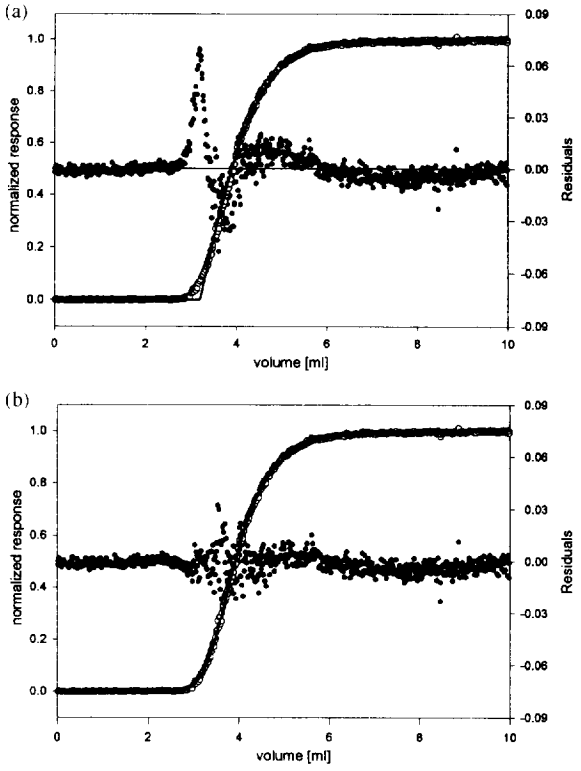

Fig. 4. Step gradients without column have been generated by a ProSys workstation. The initial buffer (buffer A) was 10 m*M* Tris–HCl at pH 8.0, the final buffer was 10 m*M* Tris–HCl + 0.5 *M* NaCl at pH 8.0. The experiment was performed at 4.0 ml/min. Open circles represent experimental data points from two consecutive runs, the solid line is the fitted curve. Closed circles indicate the residuals between fitted curve and experimental data points. (a) The response curve was fitted using Eq. (11) and (b) using Eq. (4).

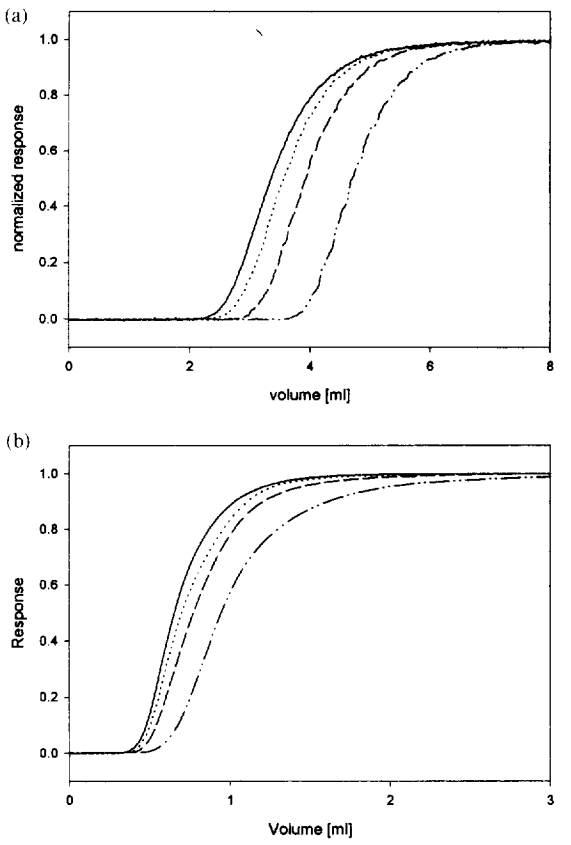

Fig. 5. Step gradients produced at flow-rates $F = 1.0$ (———), 2.0 (· · ·), 4.0 (– – –) and 8.0 ml/min (—··—··—) are superimposed. (a) Profiles from ProSys Workstation, (b) profiles from HPLC. The transition height for all experiments was kept constant as 0.5 *M* salt.

from the function obtained by fitting Eq. (4) to the experimental data set. These moments have been also correlated to flow-rate and transition height (Fig. 6e and f). Considering the logistic growth-CSTR model, the parameters a and b must be brought into a relationship with F and the transition height (Fig. 6h and i).

In Fig. 6 correlation of the aforementioned dependent variables on flow-rates and transition heights are shown. The strong dependence of the delay volume (V_D) on the flow-rate has been also statistically verified (Table 1).

This effect is caused by the delay between the signal from the software (chromatography controller), the time point when the pumps deliver the demanded liquid condition and the increase of the pulse damper volume with pressure caused by the higher flow. It is also a characteristic of the inertia of the chromatography set-up. So, the regression between V_D and F gives a time delay of 0.196±0.004 min that is 11.7±0.2 s (CI 95%). From the same regression, a dead volume of the system of 2.675 ml is calculated. The decrease of V_D with increasing transition height is only minor compared to the dependency on F but still statistically significant.

Applying a level of significance $\alpha = 0.05$ for all tests, all dependencies are significant except a corre-

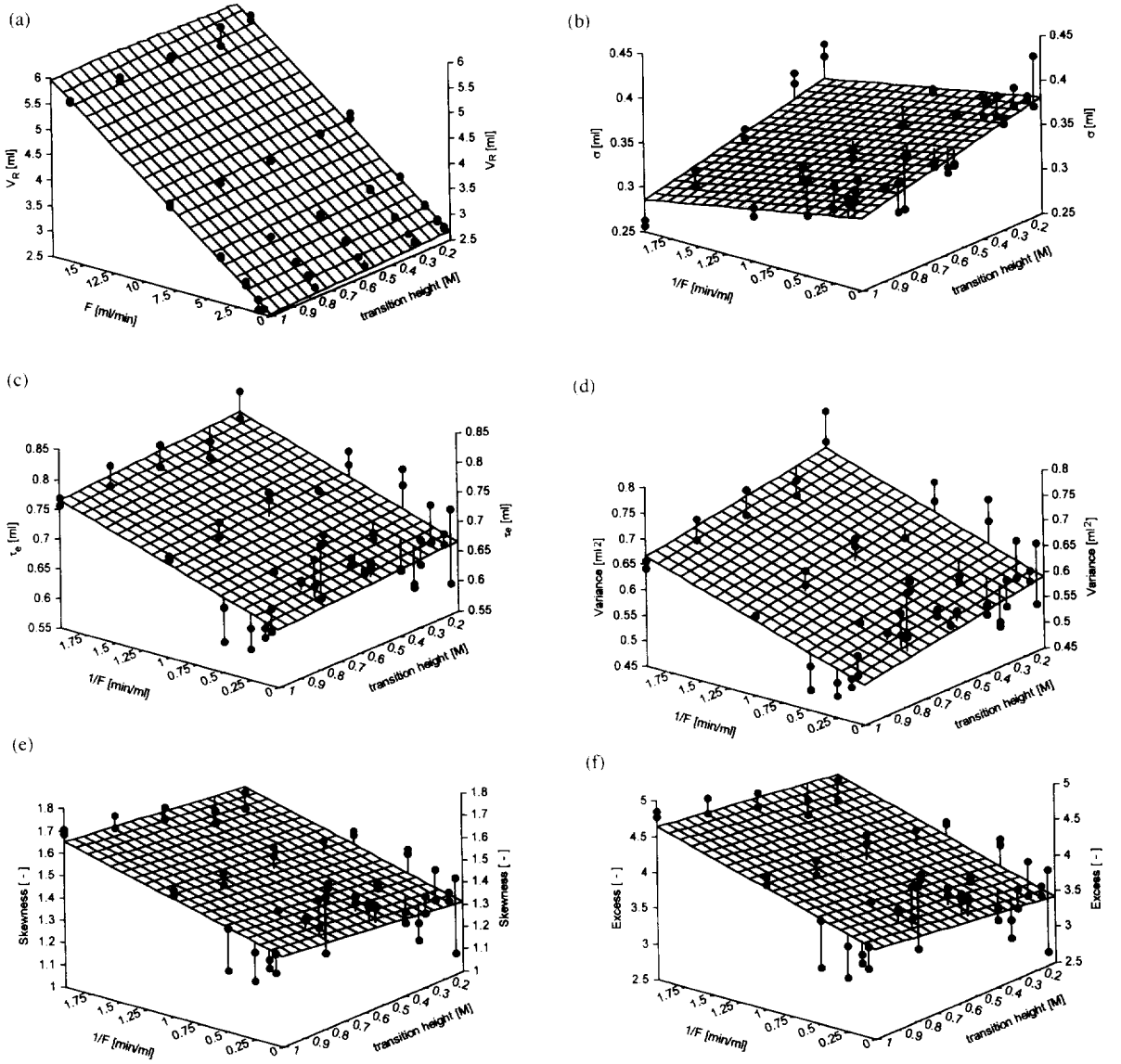

Fig. 6 (*continued overleaf*)

lation between τ_e and the transition height. Consequently, a linear regression between τ_e and $\log(F)$ was performed (Fig. 6 and Table 2).

Prediction of a step gradient using the parameter acquired before, shows a close approximation of the experimental response curve (Fig. 7). Predictions were carried out for conditions $F=2$ ml/min and a transition height of 1 *M*. The corresponding values for σ and τ_e, that are necessary to predict a response curve according to Eq. (4), were calculated from parameters given in Tables 1 and 2.

Investigation of variances (Eq. (5)), skewness (Eq. (6)) and excess (Eq. (7)) and peak asymmetry (τ/σ) concerning their dependency on F and the transition height of the salt step indicates a change of all these parameters for changing conditions (Table 3).

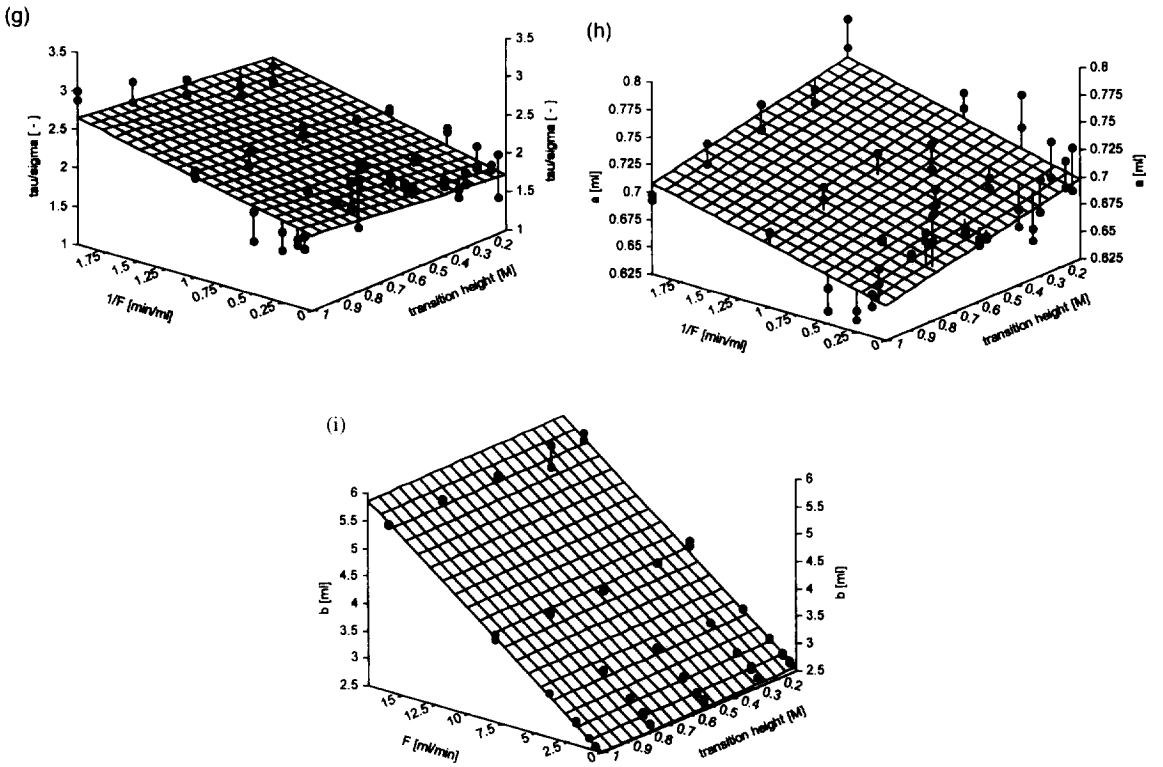

Fig. 6. Graphical representation of multiple linear regression of the independent variables flow-rate (F) and transition height and the dependent variables V_D (a), σ (b) and τ_c (c). The regression parameters corresponding to these plots are given in Table 1. For the dependent variables variance (d), skewness (e), excess (f) and the asymmetry parameter τ/σ (g) the regression parameters are given in Table 3. For the dependent parameters a (h) and b (i) the regression parameters are given in Table 4.

Table 1
Results of multiple linear regression of fitted parameters (σ, t_D, τ_c) derived by Eq. (4) using the form $Y = \text{Constant} + \text{Coefficient}_1 \cdot \text{Parameter}_1 + \text{Coefficient}_2 \cdot \text{Parameter}_2$

Y	Parameter	Coefficient	Standard error	P	R^2
V_D (ml)	Constant	2.675	0.02136	<0.0001	
	F	0.196	0.00184	<0.0001	0.995
	Transition (M)	−0.134	0.03055	<0.0001	
σ (ml)	Constant	0.3862	0.00516	<0.0001	
	$1/F$	−0.0227	0.00359	<0.0001	0.630
	Transition (M)	−0.0553	0.00747	<0.0001	
τ_c (ml)	Constant	0.6690	0.00978	<0.0001	
	$1/F$	0.0587	0.00680	<0.0001	0.578
	Transition (M)	−0.0216	0.01415	0.1326	

Correlations between the parameters and the independent variables flow-rate (F) and transition height of the step input are shown. $N = 59$; all regressions passed a normality test, a homoscedasticity test and a test of multicollinearity by a level of significance $\alpha = 0.05$.

Table 2
Results of a linear regression of τ_e versus the logarithm of F

Parameter	Coefficient	Standard error	P
Constant	0.6578	0.00648	<0.0001
$1/F$	0.0586	0.00688	<0.0001

$N=59$; the regression passed a normality test and a homoscedasticity test by a level of significance $\alpha=0.05$. $R^2=0.560$.

The variance of the applied function can be used as measure for the slope of the step gradient. The skewness is a measure how fast the step gradient reaches the plateau I_{max} and how fast the transition from I_0 to $I>I_0$ takes places. The excess reveals the deviation from the S-shaped form, either a more linear curve or a more bended one. σ/τ has a similar meaning as skewness. The statistical analysis shows that gradient shape, slope transition to I_{max} and onset depend on the transition height and the flow-rate. The delay depends also on both aforementioned variables.

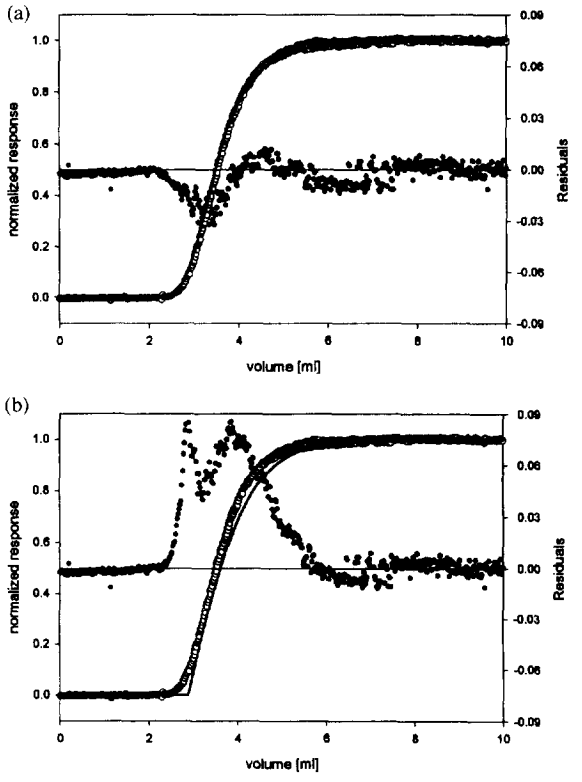

Fig. 7. Prediction of a step gradient by convolution integral method (Eq. (4)) and exponential decay expanded by logistic growth method. Parameters from Tables 1 and 2 have been used. The initial buffer was 10 mM Tris–HCl at pH 8.0, the final buffer was 10 mM Tris–HCl + 1.0 M NaCl at pH 8.0. The experiment was performed at 2.0 ml/min. Open circles represent experimental data points from two consecutive runs, the solid line is the predicted curve. Closed circles indicate the residuals between predicted curve and experimental data points. (a) Convolution integral method, (b) exponential decay expanded by logistic growth model.

Using the data set for fitting of Eq. (11) gives a similar picture (Table 4). The system delay time can be deduced from the regression between b and F and is not significantly different to the value derived from Table 1. Furthermore, the arithmetic mean of τ_e, (0.6959±0.0140) and a (0.6955±0.0080) are identical.

Additionally, Table 4 shows, that both parameters a and b are significantly correlated to F and the transition height of the salt step.

Both models are capable of describing the influence of characteristic variables on the gradient shape and the ascent delay. Considering skewness and slope both models are equivalent, although a closer investigation revealed differences in the predicted values.

Using the model in a computer-simulation program for prediction of peak profiles the influence of the salt gradient becomes obvious.

A simulation program as described by Kaltenbrunner and Jungbauer [15,16] was used. The parameters acquired for an HPLC-system as described in the method section and for the ProSys Workstation were inserted and the gradient, migration and spreading of a protein band in an ionexchanger have been calculated. A hypothetical assumption with a step function (mixer has no influence on gradient) has been compared in order to demonstrate the influence of the gradient shape on delay and band spreading (Fig. 9).

The influence of the mixing device and pre-column space inherent to a system is significant.

5. Discussion

The present considerations and theories have been only proven for chromatographic systems, which form gradients by two displacement pumps. They have not been tested with proportioning valves and

Table 3
Results of multiple linear regression using the form $Y = \text{Constant} + \text{Coefficient}_1 \cdot \text{Parameter}_1 + \text{Coefficient}_2 \cdot \text{Parameter}_2$ of variance, skewness, excess and the asymmetry parameter σ/τ calculated applying Eq. (5) to Eq. (7)

Y	Parameter	Coefficient	Standard error	P	R^2
Variance	Constant	0.5967	0.01147	<0.0001	
	$1/F$	0.0685	0.00798	<0.0001	0.617
	Transition (M)	−0.0685	0.01660	0.0001	
Skewness	Constant	1.301	0.0233	<0.0001	
	$1/F$	0.122	0.0162	<0.0001	0.547
	Transition (M)	0.107	0.0337	0.0024	
Excess	Constant	3.377	0.0821	<0.0001	
	$1/F$	0.440	0.0571	<0.0001	0.556
	Transition (M)	0.383	0.1188	0.0021	
σ/τ	Constant	1.687	0.0541	<0.0001	
	$1/F$	0.332	0.0376	<0.0001	0.623
	Transition	0.293	0.0782	0.0004	

Correlations between the parameters and the independent variables flow-rate (F) and transition height of the step input are shown. $N = 59$; all regressions passed a normality test, a homoscedasticity test and a test of multicollinearity by a level of significance $\alpha = 0.05$.

systems with syringe pumps working without pulse damper. Our buffer blending system is thought to be a stirred tank, where all mixing occurs (Fig. 2). However, in reality mixing before and after the mixing chamber occurs. Therefore this space also contributes to the mixing volume.

When step gradients are normalized in respect to the maximum salt concentration they do not appear to be identical (Fig. 3). The higher the transition height, the earlier the gradient ascends and reaches the maximum salt concentration. In order to explain this behavior, and to predict profiles two models have been developed. The first model is the convolution of the step input and exponential decay. The second model is a simple differential equation describing the effluent concentration of a stirred tank. This equation has been expanded by a function for logistic growth. It is obvious, that the actual profile of a step gradient cannot be described either by an exponential function nor a symmetrical sigmoidal function. The initial inflection of the conductivity profile occurs when the salt concentration rises and the second inflection when the ascending salt concentration approaches an asymptotic value for I_{max}. The initial inflection is much sharper. Thus, we combined the exponential decay and the logistic growth function or used the convolution integral method. As seen from Fig. 7 both models are suited

Table 4
Results of multiple linear regression of fitted parameters (a, b) derived by Eq. (11) using the form $Y = \text{Constant} + \text{Coefficient}_1 \cdot \text{Parameter}_1 + \text{Coefficient}_2 \cdot \text{Parameter}_2$

	Parameter	Coefficient	Standard error	P	R^2
a (ml)	Constant	0.7026	0.00565	<0.0001	
	$1/F$	0.0257	0.00394	<0.0001	0.566
	Transition	−0.0461	0.00817	<0.0001	
b (ml)	Constant	2.5803	0.01758	<0.0001	
	F	0.1932	0.00153	<0.0001	0.996
	Transition	−0.0944	0.02545	0.0005	

Correlations between the parameters and the independent variables flow-rate (F) and transition height of the step input are shown. $N = 59$; all regressions passed a normality test, a homoscedasticity test and a test of multicollinearity by a level of significance $\alpha = 0.05$.

to predict the gradient profiles with good approximation. The residuals between the predicted and experimental curve are smaller when the convolution integral method is utilized for prediction. The initial inflection may be accurately approximated. In the zone around the inflection point the predicted curve has a steeper slope than the experimental one. However, the second inflection and the asymptotic transition to I_{max} can be quite accurately approximated. In the case of logistic growth modified CSTR a different picture can be observed. The applied mathematical model allows only the prediction of a monotone ascending curve without an inflection point. The initial part of the curve is described by the function $f(t)=0$, when $t \leq b$. At the time point t is a sharp inflection. When $t>b$, $f(t)$ is described by the exponential function expanded by the logistic growth model (Eq. (11)). The sharp inflection is a weak point in the model, since in reality, there is a smooth transition. The residuals between experimental and predicted curve reveal this weak point. A maximum can be observed around the position which corresponds to b. Furthermore, the predicted curve is delayed with respect to the experimental values. At the time span between the inflection point and the transition to the maximal salt concentration a second peak in the residuals between experimental and predicted curve can be observed. Responsible for this result is parameter b. Its estimation is too high, since positive residuals appear in the time span when dI/dt is high ($I=0.1$–0.9). Residuals at the onset of the ascent are due to the inadequacy of the model as it has been mentioned before.

Correlation of the estimated parameters to F and transition height provide a quantitative insight how gradients will change with those variables. It is interesting to note that the delay volume V_D is inversely proportional to the transition height, but highly dependent on F. A possible explanation for this observation is the different pressure drop within the system produced by different viscosities and/or densities of the solutions. The increasing delay V_D with increasing F indicates that the system volume changes. The higher F the more pressure is on the elastic membrane of the pulse damper and subsequently due to the extension of the membrane the system volume increases. The HPLC displacement pumps require a pulse damper in order to compensate the oscillating flow and pressure. Parameter b of the logistic growth–CSTR model has a similar meaning as V_D. A similar relationship between b and F and b and transition height can be observed. Therefore, attention must be paid when a method is transferred to an other type of equipment. The gradient shape will change with the stock solutions as well as the equipment used for buffer blending. For example, the gradient shape is different, if a 250 mM step gradient is made from a 0.5 M NaCl or a 2.0 M NaCl stock solution.

Front shape and delay are strongly dependent upon F. The correlation of variance, skew and excess with F and the transition height exhibits this strong dependence of the front shape on F. In order to avoid misinterpretations, the peak parameters variance, skew and excess are used to describe the gradient shape. As an example, if cumulative error functions (with 3 different τ/σ values) are superimposed on a graph, the influence of τ/σ becomes obvious (Fig. 8). The upper part of the curve is especially susceptible to the changes in the τ/σ ratio.

As the flow-rate becomes bigger τ_e decreases. This phenomenon shows that washing out is more effected by the flow-rate the increase of the system volume by the increased flow. τ/σ shows the step gradient becomes a steeper transition with flow-rate and the maximum salt concentration is reached faster with low transition height. In principle all step gradients have a S-shaped curve. A closer view shows that this curve varies with the input variable F and transition height. Variance is negatively correlated with transi-

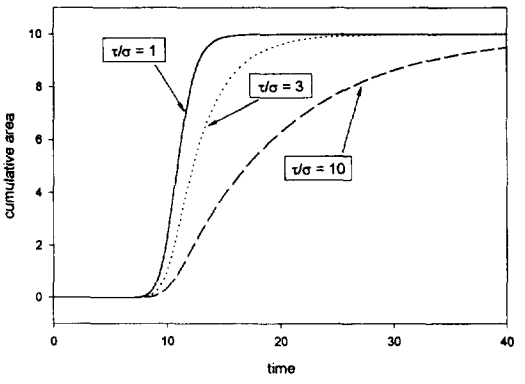

Fig. 8. Cumulative functions of a exponential modified Gaussian function with different τ/σ ratio. An arbitrary area of 10, amplitude of 10 and variance of 1 have been chosen.

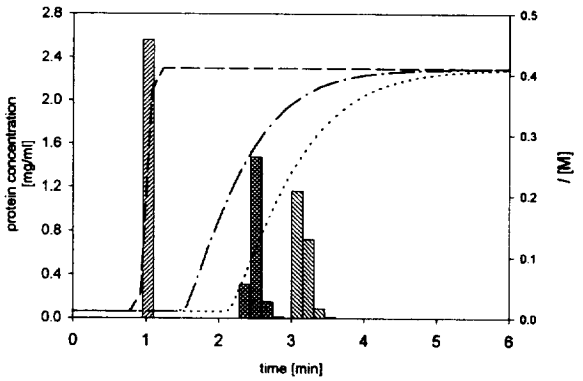

Fig. 9. Comparison of predictions of three different experimental setups. The bar graph represents the protein concentration and the line graph the salt concentration. A hypothetical model without a mixer (bar on the left and ——), a HPLC system (bars in the middle and —·—·—) and a ProSys Workstation (bars on the right and · · ·) are compared. The simulation was carried out according to Jungbauer and Kaltenbrunner [15] using following conditions: column: $d=0.5$ cm; $L=5$ cm; Np=32; Nps=40; $\epsilon=0.47$. Gradient: $I_0=0.01$ M, $I_{elu}=0.41$ M, step gradient, $F=1.0$ ml/min, Sample: $C_0=20$ mg/ml, $V_S=0.02$ ml. The adsorption isotherm was a Freundlich isotherm with asymmetric logistic dose response with following parameters: $a=241.063$; $b=0.766071$; $c=2.58254$; $d=122.096$; $e=0.0357043$.

tion height. The higher transition from I_0 to I_{max}, the lower the variance. The gradient becomes steeper and the transition is completed within a smaller time span. The real shape comes closer to the step function. Skew reveals that the transition to I_{max} is very slow. The positive excess shows a quite prominent deviation from the S-shaped form.

The aforementioned analysis allows us to conclude that the higher the concentration difference between two solutions, the faster the breakthrough of the salt front. The delay time b is decreasing with increasing step height while the exponential time constant a is increasing. This effect can be implemented in a model for simulation of step gradients in preparative chromatography. When two chromatographic systems are compared, the influence of the gradient shape becomes unmistakable (Fig. 9). The delay time of the protein band as well as the peak width are influenced. Computer simulation of preparative chromatography without considering the contribution of the mixing device cannot approximate realistic conditions.

The model can be used for scale-up and scale-down studies and for validation of chromatographic systems.

Acknowledgments

We want to acknowledge the helpful discussion with Tim Warner.

References

[1] A. Jungbauer, J. Chromatogr., 639 (1993) 3.
[2] E. Wisniewski, BioSeparation, 3 (1992) 77.
[3] E. Wisniewski, E. Boschetti and A. Jungbauer, in K.E. Avis and V.L. Wu (Editors), Biotechnology and Pharmaceutical Manufacturing, Processing and Preservation, Interpharm Press, Buffalo Grove, IL, 1996, Ch. 3, p. 61.
[4] A. Jungbauer, Curr. Opin. Biotechnol., 7 (1996) 210.
[5] J.L. Glaich and L.R. Snyder (Editors), Computer-Assisted Method Development for High-Performance Liquid Chromatography, Elsevier, Amsterdam, 1990; J. Chromatogr., Vol. 485 (1989).
[6] J.C. Bellot and J.S. Condoret, Proc. Biochem., 26 (1991) 363.
[7] J.C. Bellot and J.S. Condoret, Proc. Biochem, 28 (1993) 365.
[8] O. Kaltenbrunner, A. Jungbauer and S. Yamamoto, J. Chromatogr. A, in press.
[9] J.C. Sternberg, Adv. Chromatogr., (1966) 205.
[10] O. Grubner, Adv. Chromatogr., (1968) 173.
[11] E. Grushka, Anal. Chem., 44 (1972) 1733.
[12] J.Å. Jönsson (Editor), in Chromatographic Theory and Basic Principles, Marcel Dekker, New York, 1987, Ch. 2, p. 27.
[13] K. Yamaoka and T. Nakagawa, J. Chromatogr., 100 (1974) 1.
[14] M. Abromovitz and I.A. Stegun, Handbook of Mathematical Functions, Dover, New York, 1965.
[15] A. Jungbauer and O. Kaltenbrunner, Biotechnol. Bioeng., 52 (1996) 223.
[16] O. Kaltenbrunner and A. Jungbauer, J. Chromatogr. A, 734 (1996) 183.